EQUATION OF STATE OF SOLIDS: ALUMINUM AND TEFLON

G. D. Anderson

D. G. Doran

A. L. Fahrenbruch

Stanford Research Institute
Menlo Park, California
Contract AF?9(601)-6409

TECHNICAL REPORT NO. AFWL-TR-65-147

December 1965

AIR FORCE WEAPONS LABORATORY
Research and Technology Division
Air Force Systems Command
Kirtland Air Force Base
New Mexico

AFWL-TR-65-147

EQUATION OF STATE OF SOLIDS: ALUMINUM AND TEFLON

Final Report

G. D. Anderson

D. G. Doran

A. L. Fahrenbruch

Stanford Research Institute
Menlo Park, California
Contract AF29(601)-6409

TECHNICAL REPORT NO. AFWL-TR-65-147

FOREWORD

This report was prepared by Stanford Research Institute, Menlo Park, California, under Contract AF29(601)-6409. The work was performed under Program Element 7.60.06.01.D, Project 5710, Subtask 15.018, and was funded by the Defense Atomic Support Agency (DASA).

Inclusive dates of research were 15 May 1964 through 14 July 1965. The report was submitted 12 November 1965 by the AFWL Project Officer, Lt Raymond J. Lawrence, Jr., (WLRP).

This report has been reviewed and is approved.

RAYMOND J. LAWRENCE, JR.
1Lt USAF
Project Officer

CLYDE C. REYNOLDS
Lt Colonel USAF
Chief, Physics Branch

WILLIAM H. STEPHENS
Colonel USAF
Chief, Research Division

ABSTRACT

Pressure, volume, and energy equation of state data obtained using shock wave techniques are presented for aluminum and Teflon. Solid aluminum samples initially at room temperature or preheated to near melting, and porous aluminum samples at room temperature, were studied over a pressure range of 200 to 1200 kbar. It was found that the largest variations of volume and energy could be achieved using porous samples. Values of Grüneisen's ratio estimated from values of the thermal pressure and thermal energy range from 2.1 to 1.37. Due to the sensitivity of Grüneisen's ratio to the Hugoniot data, it is not possible to formulate its energy or volume dependence conclusively at the present time. Of greatest significance is the fact that it does not vary widely.

Solid and porous Teflon samples were studied over a pressure range of 100 to 500 kbar. Hugoniot curves drawn on the basis of the ten data points obtained indicate a variation of Grüneisen's ratio from about 0.7 to 2.0.

CONTENTS

ILLUSTRATIONS

TABLES

SECTION I

INTRODUCTION

Calculations describing wave propagation in a continuous medium require the knowledge of a constitutive relation or equation of state characterizing the material properties of the medium. In solids at pressures greatly in excess of the shear yield stress, an equation of state relating pressure, volume, and internal energy sufficiently describes the medium. The work reported here was undertaken to study the equation of state of aluminum and Teflon using shock-wave techniques. The largest portion of the effort was spent investigating aluminum. In order to reach thermodynamic states lying in a region of the pressure-volume plane rather than along a single Hugoniot curve, the initial state of the material must be varied. This variation was achieved by using solid and porous aluminum at room temperature and by preheating solid aluminum to several hundred degrees prior to shocking. It was found that the largest changes in the final shock state could be produced using porous samples.

The following sections include a general discussion of equations of state of simple systems and how they may be studied by shock waves, a description of the experimental techniques used and the performance of the experiments, and an analysis of the data and comparison with other data and equations of state.

SECTION II

BASIC THERMODYNAMICS OF SHOCK WAVES

1. EQUATIONS OF STATE

The term "equations of state" has unfortunately been used in shock wave literature to denote a variety of relationships which convey different amounts of thermodynamic information about the system under consideration. Quite frequently curves such as isentropes, adiabats, or Hugoniots are referred to as equations of state. The specification of one of these curves is not a specification of the equation of state of the system because an equation of state is a function of at least two independent variables. The purpose of this section is to summarize the basic thermodynamics of equations of state of simple, nonreacting, single phase systems.

In a simple system the two independent variables are generally taken to be any two of the four variables volume, pressure, temperature, and entropy, denoted by V, P, T, and S, respectively. Expressions for the remaining two as functions of the two so chosen constitute a complete equation of state, since they yield a complete thermodynamic description of the system. Each of the relationships independently is called an incomplete equation of state, or simply equation of state. Given the two relationships, $T = T(S,V)$, $P = P(S,V)$, which can in principle be inverted so that any pair of variables is independent, the internal energy is given by

$$dE = TdS - PdV \tag{1}$$

Knowledge of the internal energy $E(S,V)$ is then equivalent to the two equations of state $T(S,V)$ and $P(S,V)$ since

$$T(S,V) = \left(\frac{\partial E}{\partial S}\right)_V, \quad P(S,V) = -\left(\frac{\partial E}{\partial V}\right)_S \tag{2}$$

The function $E(S,V)$ is frequently called a fundamental equation or complete equation of state because it also contains a complete thermodynamic

description of the system. If V and T are chosen as independent variables, then $S(V,T)$ and $P(V,T)$ form a complete equation of state. Analogous to Eq. (1), the Helmholtz free energy is given by

$$dF = -SdT - PdV \tag{3}$$

and $F(V,T)$ is the fundamental equation equivalent to the two equations of state $S(V,T)$ and $P(V,T)$ since

$$S(V,T) = -\left(\frac{\partial F}{\partial T}\right)_V, \quad P(V,T) = -\left(\frac{\partial F}{\partial V}\right)_T \tag{4}$$

Similarly the enthalpy function $H(S,P)$ and the Gibbs free energy $G(P,T)$ serve as fundamental equations when the independent variables are the pairs (S,P) and (P,T) respectively. Complete equations of state may be formulated in other ways; all formulations of a complete equation of state are equivalent and can be deduced one from another through general thermodynamic relationships.

Quite frequently one of the incomplete equations of state is the internal energy $E(V,T)$ or $E(P,V)$. Recall that the internal energy is a complete equation of state or fundamental equation only when it is expressed as a function of S and V. If $E(V,T)$ is known, supplementing it with either $P(V,T)$ or $S(V,T)$ constitutes a complete equation of state[1]. Similarly supplementing $E(P,V)$ with either $T(P,V)$ or $S(P,V)$ constitutes a complete equation of state[1].

In shock wave research the incomplete equation of state $E(P,V)$ is of particular interest. This equation of state involves only the mechanical thermodynamic variables P, V, and E and does not yield values of the thermal thermodynamic variables S and T. Shock wave measurements yield an $E(P,V)$ incomplete equation of state since the values of pressure, volume, and energy are computed from the Rankine-Hugoniot jump conditions expressing the conservation of mass, momentum, and energy, that do not involve the entropy and temperature explicitly.

[1] If one is known, the other can be determined in principle from Eq. (1).

Let us then summarize. In a simple thermodynamic system there are two independent variables. These two are generally chosen from V, T, S, and P. An equation expressing one of the remaining pair as functions of the independent variables is called an incomplete equation of state. Expression of both remaining variables in terms of the two independent variables is a complete equation of state, *i.e.*, a set of relationships from which all other thermodynamic properties of the system can in principle be computed. The internal energy may be added to the above quartet of variables, but it is related to them through Eq. (1). An isentrope is the intersection of the incomplete equation of state surface $P = P(S,V)$ with a plane S = constant. Thus, prescribing an isentrope $P = P(S_0,V) = f(V)$ is not prescribing an equation of state. Similarly a Hugoniot curve is obtained by subjecting an $E(P,V)$ incomplete equation of state to the constraint

$$E(P,V) = E_0 + \frac{1}{2}(P_0 + P)(V_0 - V)$$

where $E_0 = E(P_0,V_0)$. Specifying a Hugoniot curve is not specifying an equation of state of the system.

2. MIE-GRÜNEISEN EQUATION OF STATE

It was stated earlier that equation of state information obtained from shock wave data leads to an incomplete equation of state of the type $E(P,V)$ This equation of state tells the value of the internal energy of the system over a region of the pressure-volume plane but does not contain the information necessary to compute the temperature or entropy in the same region. Since temperature and entropy are thermal thermodynamic variables, as contrasted to pressure and volume which are mechanical thermodynamic variables, the $E(P,V)$ equation of state might be suitably called a mechanical equation of state. The energy, pressure, and volume are obtained from shock data by measuring wave velocities and applying the Rankine-Hugoniot jump conditions expressing conservation of mass, momentum, and energy.

In problems of flow calculations the incomplete $E(P,V)$ equation of state may be sufficient since it does permit calculation of the curves of constant entropy in the pressure-volume plane. The constant value of the entropy associated with each isentrope is unknown, however. One P-V-E equation of state which has been extensively used in describing

metals is the Mie-Grüneisen equation of state with the Grüneisen ratio Γ assumed to be a function of volume only. In general the Grüneisen parameter, as for all thermodynamic state variables, is a function of two independent variables and is defined by

$$\Gamma(X,Y) = V\left(\frac{\partial P}{\partial E}\right)_V = V\,\frac{(\partial P/\partial T)_V}{(\partial E/\partial T)_V} = V\,\frac{(\partial S/\partial V)_T}{T(\partial S/\partial T)_V} \tag{5}$$

where X and Y represent any two of the five variables E, P, S, V, and T which are chosen as independent. We shall define the generalized Mie-Grüneisen equation of state as the solution of any one of the partial differential equations of Eq. (5) when $\Gamma(X,Y)$ is specified All of the definitions of Eq. (5) are equivalent and may be derived one from another by applying thermodynamic identities.

Using the last definition of Eq. (5),

$$\frac{V}{\Gamma(V,T)}\left(\frac{\partial S}{\partial V}\right)_T - T\left(\frac{\partial S}{\partial T}\right)_V = 0 \tag{6}$$

Along an isentrope $S(V,T)$ = constant and

$$dS = \left(\frac{\partial S}{\partial V}\right)_T dV + \left(\frac{\partial S}{\partial T}\right)_V dT = 0 \tag{7}$$

Therefore the isentropes in the V-T plane are given by the integrals of

$$\left(\frac{\partial T}{\partial V}\right)_S = -\frac{\Gamma(V,T)}{V} \tag{8}$$

The usual Mie-Grüneisen equation of state as applied to solids is obtained by writing the pressure and internal energy each as a sum of 0°K compressional component and a thermal component:

$$\begin{aligned} E(V,T) &= E_c(V) + E_{th}(V,T) \\ P(V,T) &\quad P_c(V) + P_{th}(V,T) \end{aligned} \tag{9}$$

where $P_c(V) = -dE_c(V)/dV$, the subscript c refers to 0°K, and the thermal components vanish for all V at $T = 0$. Also the Grüneisen parameter Γ is

taken to be a function of volume alone, *i.e.*, $\Gamma \equiv \Gamma(V)$. In this case integration of Eq. (8) yields

$$T = \Phi(S)\theta(V) \tag{10}$$

where

$$\theta(V) = \theta_0 e^{-\int \frac{\Gamma(V)}{V} dV} \tag{11}$$

and $\Phi(S)$ is function of the entropy and hence constant along an isentrope. The thermodynamic definition of the temperature combined with Eq. (10) gives

$$T(S,V) = \left(\frac{\partial E}{\partial S}\right)_V = \Phi(S)\theta(V) \quad . \tag{12}$$

Integration of Eq. (12) then yields

$$E(S,V) - E_c(V) = \theta(V) \int_0^S \Phi(S) dS \tag{13}$$

since $E(O,V) \equiv E_c(V)$. Equation (13) is a fundamental equation since it expresses the internal energy E as a function of S and V. This equation can be evaluated explicitly as a function of S and V if the functions $E_c(V)$, $\Phi(S)$, and $\theta(V)$ or $\Gamma(V)$ are known. Thus, for a system in which Γ is a function of volume only, the specification of $E_c(V)$, $\Gamma(V)$, and $\Phi(S)$ constitutes a complete equation of state. The pressure is given by

$$P(S,V) = -\left(\frac{\partial E}{\partial V}\right)_S = -\frac{dE_c(V)}{dV} - \frac{d\theta(V)}{dV} \int_0^S \Phi(S) dS \tag{14}$$

But $-dE_c(V)/dV = P_c(V)$ and therefore

$$P(S,V) = P_c(V) + \frac{\Gamma(V)\theta(V)}{V} \int_0^S \Phi(S) dS$$

$$= P_c(V) + \frac{\Gamma(V)}{V} [E(S,V) - E_c(V)] \quad , \tag{15}$$

where Eqs. (11) and (13) have been used. Eq. (15) is the usual Mie-Grüneisen equation of state and does not require knowledge of the entropy through $\Phi(S)$.

Equation (15) could have been obtained by direct integration of the first form of Eq. (5). However, this method shows what information is needed to form a complete equation of state and how the E-P-V equation does not depend upon entropy.

Consider now the specific heat at constant volume as a function of T and V. The change in $C_V(V,T)$ along an isentrope is given by

$$\left(\frac{\partial C_V}{\partial V}\right)_S = \left(\frac{\partial C_V}{\partial V}\right)_T + \left(\frac{\partial C_V}{\partial T}\right)_V \left(\frac{\partial T}{\partial V}\right)_S$$

$$= T\left[\frac{\partial}{\partial V}\left(\frac{\partial S}{\partial T}\right)_V\right]_T - \left(\frac{\partial C_V}{\partial T}\right)_V \left(\frac{\partial P}{\partial S}\right)_V \quad , \tag{16}$$

using $C_V = T(\partial S/\partial T)_V$ and $(\partial T/\partial V)_S = -(\partial P/\partial S)_V$. Furthermore, since $T = (\partial E/\partial S)_V$ and $(\partial P/\partial T)_V = (\partial S/\partial V)_T$,

$$\left(\frac{\partial C_V}{\partial V}\right)_S = T\left[\frac{\partial}{\partial T}\left(\frac{\partial S}{\partial V}\right)_T\right]_V - \left(\frac{\partial C_V}{\partial T}\right)_V \frac{(\partial P/\partial E)_V}{(\partial S/\partial E)_V}$$

$$= T\left[\frac{\partial}{\partial T}\left(\frac{\partial P}{\partial T}\right)_V\right]_V - T\left(\frac{\partial C_V}{\partial T}\right)_V \left(\frac{\partial P}{\partial E}\right)_V \quad . \tag{17}$$

$$T\left[\frac{\partial}{\partial T}\frac{(\partial P/\partial E)_V}{(\partial T/\partial E)_V}\right]_V - T\left(\frac{\partial C_V}{\partial T}\right)_V \left(\frac{\partial P}{\partial E}\right)_V = T\left\{\left[\frac{\partial}{\partial T} C_V \left(\frac{\partial P}{\partial E}\right)_V\right]_V - \left(\frac{\partial C_V}{\partial T}\right)_V \left(\frac{\partial P}{\partial E}\right)_V\right\}$$

$$= TC_V\left[\frac{\partial}{\partial T}\left(\frac{\partial P}{\partial E}\right)_V\right]_V = C_V\left(\frac{\partial \Gamma}{\partial T}\right)_V \tag{18}$$

If Γ is a function of volume only, Eq. (18) shows that $C_V(V,T)$ is constant along an isentrope. Thus $C_V(V,T) \equiv C_V[\psi(S)]$ is some function of the entropy only. Eq. (9) implies that when Γ is a function of volume only,

$$S \equiv f\left(\frac{\theta(V)}{T}\right) \tag{19}$$

Thus for $\Gamma = \Gamma(V)$ the specific heat at constant volume is given by

$$C_V(V,T) \equiv g\left(\frac{\theta(V)}{T}\right) \tag{20}$$

One special case of interest is the Debye model of a solid. A result of this model is that the specific heat at constant volume is a function of $\theta_D(V)/T$ where $\theta_D(V)$ is the Debye characteristic temperature. Identifying $\theta_D(V)$ from the Debye model with $\theta(V)$ in Eq. (20) and using Eq. (10) yields a relationship between Grüneisen's ratio $\Gamma(V)$ for a Debye solid with the Debye temperature $\theta_D(V)$

$$\Gamma(V) = \frac{d\ ln\ \theta_D(V)}{d\ ln\ V} \tag{21}$$

Slater (Ref. 1) suggested a relationship between $\Gamma(V)$ and the isentropes of the system based on the Debye model and the assumption that in an elastic solid the ratio of the longitudinal sound speed to the transverse or shear sound speed is independent of volume. This assumption is equivalent to assuming that the ratio of the isentropic bulk modulus to the isentropic rigidity modulus is volume independent or that Poisson's ratio is volume independent. The Debye characteristic temperature is given by (Ref. 1):

$$\theta_D(V) = A\left[\frac{2V}{2C_l^3 + C_T^3}\right]^{-1/3} \tag{22}$$

where C_L and C_T are the longitudinal and transverse sound wave velocities respectively and A is a constant.

$$ln\ \theta_D = ln\ A - \frac{1}{3}\ ln\ 2V + ln\ C_L + \frac{1}{3}\ ln\ (2 + C_T^3/C_L^3) \tag{23}$$

$$\frac{d\ ln\ \theta_D}{d\ ln\ V} = -\frac{1}{3} + \frac{d\ ln\ C_L}{d\ ln\ V} \tag{24}$$

where it has been assumed that $C_T/\ C_L$ is independent of volume. The longitudinal elastic wave velocity is given by

$$C_L = [V(K + \frac{4}{3}\mu)]^{1/2} \tag{25}$$

where K is the isentropic bulk modulus and μ is the rigidity modulus.

$$ln\ C_L = \frac{1}{2}\ ln\ V + \frac{1}{2}\ ln\ K + \frac{1}{2}\ ln\left(1 + \frac{4\mu}{3K}\right) \tag{26}$$

Since the assumption C_T/C_L is independent of volume implies μ/K is independent of volume,

$$\frac{d\ ln\ C_L}{d\ ln\ V} = \frac{1}{2} + \frac{1}{2}\ \frac{d\ ln\ K}{d\ ln\ V} \tag{27}$$

Now

$$K = V\left(-\frac{\partial P}{\partial V}\right)_S \tag{28}$$

$$\frac{d\ ln\ C_L}{d\ ln\ V} = \frac{1}{2} + \frac{V}{2}\ \frac{(\partial^2 P/\partial V^2)_S}{(\partial P/\partial V)_S} \tag{29}$$

Combining Eqs. (29) and (24) yields

$$\Gamma(V) = -\frac{d\ ln\ \theta_D}{d\ ln\ V} = -\frac{V}{2}\ \frac{(\partial^2 P/\partial V^2)_S}{(\partial P/\partial V)_S} - \frac{2}{3} \tag{30}$$

This is the Slater relation for Grüneisen's ratio in terms of the derivatives of the isentropes. It has been derived on the basis of the Debye model and the assumption that the ratio of the sound speeds is independent of volume. Since Γ has been assumed dependent on volume only, the ratio of the partial derivatives on the right hand side of Eq. (30) is also dependent on volume only, that is, independent of entropy. Since the relation must hold then on any isentrope at a given volume, it must hold on the isentrope $S = 0$ which is also the isotherm $T = 0$.

Dugdale and MacDonald (Ref. 2) propose that the Slater relation be modified to

$$\Gamma(V) = -\frac{V}{2}\ \frac{\partial^2(PV^{2/3})/\partial V^2}{\partial(PV^{2/3})/\partial V} - \frac{1}{3} \tag{31}$$

where again P refers to the isotherm $T = 0°K$. The Dugdale-MacDonald relation has been used in extensive calculations by Rice, McQueen, and Walsh (Ref. 3) based on shock data.

In summary, the usual form of the Mie-Grüneisen equation of state is that of Eq. (15), which is a consequence of assuming $\Gamma = \Gamma(V)$. If the Debye model of a solid is used, $\Gamma(V)$ and the Debye characteristic temperature are related by Eq. (21). Substitution of the expression for the Debye temperature, Eq. (22), into Eq. (21) plus the assumption of constant Poisson's ratio, yields the Slater relation between $\Gamma(V)$ and the 0°K isotherm.

Equation (15) may be written

$$P - P_c(V) = \frac{\Gamma(V)}{V} [E - E_c(V)] \tag{15}$$

The point P, V, E refers to any arbitrary equilibrium state in the region of the pressure-volume plane for which Eq. (15) is valid. $P_c(V)$ and $E_c(V)$ are the compressional pressure and energy at that same volume. Equation (15) says, then, that the thermal component of the pressure at volume V is equal to $\Gamma(V)/V$, a function of volume, times the thermal component of the energy at the same volume. In particular, if the pressure-volume, energy state under consideration lies on a Hugoniot curve centered on state P_0, V_0, E_0, Eq. (15) becomes

$$P_H - P_c(V) = \frac{\Gamma(V)}{V} [E_H - E_c(V)] \tag{32}$$

Subtraction of Eq. (32) from Eq. (15) yields

$$P - P_H = \frac{\Gamma(V)}{V} [E - E_H] \tag{33}$$

Equation (33) now says that at volume V the difference in thermal pressure between the state P, V, E and the Hugoniot centered at P_0, V_0, E_0 is equal to $\Gamma(V)/V$ times the difference in thermal energy between state P, V, E and the Hugoniot. Since 0°K isotherms are not directly measurable as are Hugoniot curves, it is convenient to use the equation of state in the form of Eq. (33) with the Hugoniot as a reference. If $\Gamma(V)$ is assumed to have a constant value G and the experimental Hugoniot is expressed as a function of $\mu = (\rho/\rho_0) - 1$, Eq. (33) can be written

$$P = P_H(\mu) + G\rho E' \tag{34}$$

where $\rho = 1/V$ and $E' = E - E_H$, the thermal energy offset from the Hugoniot. The Hugoniot internal energy and pressure are related through

$$E_H = E_0 + \frac{1}{2} P_H(V_0 - V)$$

$$= E_0 + \frac{\mu P_H}{2\rho} \tag{35}$$

Substitution of Eq. (35) into (34) yields

$$P = P_H(\mu)\left[1 - \frac{G\mu}{2}\right] + G\rho(E - E_0) \tag{36}$$

where E is the total internal energy and E_0 is the internal energy at the foot of the Hugoniot $P_H(\mu)$. Equation (36) is valid for $G(\mu)$ as well as G constant. However, if G or Γ were to have an energy or temperature dependence, the P-V-E equation of state would not have had the form of Eq. (15) which led to Eq. (36). If Γ is a function of the energy as well as volume, the generalized Mie-Grüneisen equation of state is given by integration of the differential equation (5) defining $\Gamma(E,V)$. Taking E and V as independent variables

$$\Gamma(E,V) = V\left(\frac{\partial P}{\partial E}\right)_V \tag{5}$$

Integrating at constant V

$$P - P_r(V) = \frac{1}{V}\int_{E_r(V)}^{E} \Gamma(E,V)\,dE \tag{37}$$

where $E_r(V)$ and $P_r(V)$ are the energy and pressure at some reference point at the volume V.

3. SHOCK WAVE MEASUREMENTS OF EQUATION OF STATE

A series of experiments, in which shock waves of varying intensity are produced in a material and measurements of the resulting shock and particle velocities are made, yields a single Hugoniot curve uniquely specified by the initial state. The specific volume V and pressure P

are related to the shock and particle velocities through the equations

$$\frac{V}{V_0} = 1 - \frac{u}{U} \tag{38}$$

and

$$P = \rho_0 U u$$

which express the conservation of mass and momentum, respectively. The energy along the Hugoniot curve is given by

$$E = E_0 + \frac{1}{2} P(V_0 - V) \tag{40}$$

where E_0 is the energy at $P = 0$, $V = V_0$. As stated earlier, a single Hugoniot curve is not an equation of state; it is only a particular pressure-volume curve along which the energy can be computed from Eq. (40). A P-V-E equation of state consists of knowing the energy over a region of the P-V plane. For each initial state there exists a different Hugoniot curve. Therefore, by varying the initial state of a system, shock-wave experiments can be used to generate many Hugoniot curves in the P-V plane which then may be used to infer the dependence of the internal energy on volume and pressure.

In the work to be described, preheated material, porous material, and multiple shocks have been used to vary the initial state. The preheating technique consists of initially heating the material, aluminum in this case, at zero pressure to near its melting point. The initial volume increases due to thermal expansion and the initial energy increases by an amount $\Delta E = \int C_p dT$. The double shocking technique consists of reflecting the initial shock induced in the material from a material of high shock impedance, tungsten for example. The state behind the first shock then serves as an initial state for the reflected second shock. The use of porous materials, described first in the open literature by the Russians (Ref. 4), produces a large increase of thermal internal energy in the sample during shock compression due to the irreversible collapse of the porous structure. Due to the large thermal energies, Hugoniot curves of both positive and negative slopes are observed. (Refs. 5, 6, 7) Such behavior of the Hugoniot curves of metals can be explained by using the ordinary Mie-Grüneisen equation of state with $\Gamma = \Gamma(V)$ or a more elaborate equation of state taking account of the thermal contribution of the conduction electrons.

SECTION III

EXPERIMENTAL TECHNIQUE

To obtain Hugoniot points for aluminum which do not all lie on a single curve the three approaches described in Section II of this report have been attempted. These are single shocking porous material, double shocking porous material, and preheating the material; only the first method was used extensively. In studying Teflon, the first method was used exclusively. In this portion of the report are described sample preparation and experimental technique.

1. METHOD OF OBTAINING HUGONIOT DATA

Hugoniot points were determined by the impedance match method (Ref. 3), using 2024 aluminum as a standard, as illustrated below for a porous aluminum specimen. At the driver-porous aluminum interface a shock is transmitted into the porous aluminum and a rarefaction is reflected back into the 2024 driver. Since the Hugoniot and relief isentrope cross curves in the pressure (P)-particle velocity (u) plane for 2024 aluminum are known, (Refs. 3,8) a measurement of the free-surface velocity of the 2024 driver and the shock velocity through the sample suffice to fix a point on the Hugoniot of the sample. The measurement of the driver free-surface velocity gives the point C on the P-u diagram of figure 1, indicating that the initial shock state in the driver is state B. All of the states which the 2024 can reach from state B through a reflected

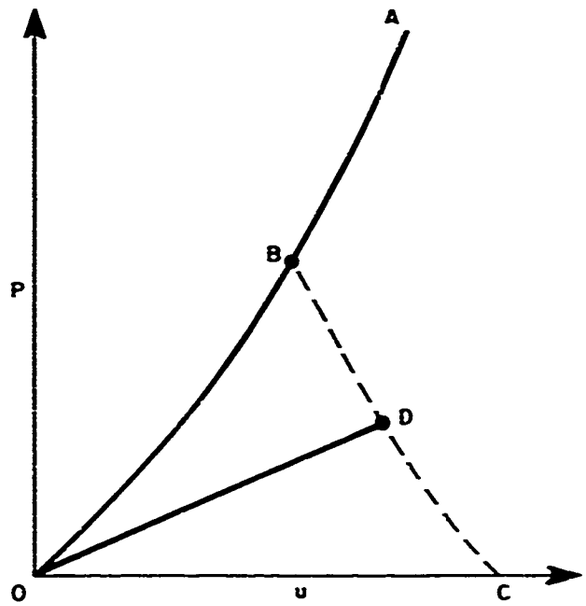

FIG. 1 IMPEDANCE MATCH METHOD OF DETERMINING A HUGONIOT

isentropic rarefaction lie on the cross surve *CDB*. Since there must be continuity of pressure and particle velocity at the 2024-porous aluminum interface, the shocked state in the porous aluminum must also lie on this cross curve. Equation (39) requires that the Hugoniot point of the porous material lies on a ray through the origin of slope $\rho_0 U/m$, where m is the porosity, ρ_0 is the crystal density of aluminum, and U is the shock velocity through the sample. Hence the intersection of this ray, *OD*, with the cross curve, *CDB*, yields a point on the Hugoniot of porous aluminum.

2. DESCRIPTION OF EXPERIMENTS

a. Room Temperature Shots

Shocks were induced into 2024 aluminum drivers, upon which the samples were mounted, by high explosive in direct contact or by the impact of an explosively accelerated flying plate. The direct contact driver system consisted of an 8-inch-diameter plane wave lens[2] initiating a pad of 9404 HE, 4 inches long and 8 inches in diameter, in contact with a 3/8- or 1/2-inch-thick 2024 aluminum driver plate.

Most of the experiments required flying-plate systems because of the high pressures desired. The samples were mounted on a 3/8- or 1/4-inch-thick 2024 aluminum driver plate. A strong shock wave was produced in the driver by impact of a 1/8- or 3/16-inch-thick stainless steel or brass flyer plate (see figure 2). In all cases an 8-to-9-inch-diameter explosive pad, initiated by a plane wave lens, was used to accelerate the flyer plate across a 3/4-inch or 1-inch air gap. To prevent spalling and breakup of the flyer, it was separated from the explosive pad by a 1/16-inch Plexiglas buffer.

All velocities were determined by optical techniques with a rotating mirror streak camera at a writing speed of 3.78 mm/μsec. Multiple slits were used and illumination was by an explosive argon light source. Measurement of shock velocity through the samples was made by small glass mirrors bonded to the driver free surface and aluminized Mylar bonded to the steel rings in which the porous samples were pressed. Destruction of the mirrors on the driver surface gave the arrival time of the shock at the driver-sample interface and the destruction of the Mylar gave the arrival time of the shock at the sample free surface.

Measurement of the free-surface velocity of the 2024 aluminum driver plate is made by mounting a mirror inclined at a small angle on the driver

[2] P-80, Pantex.

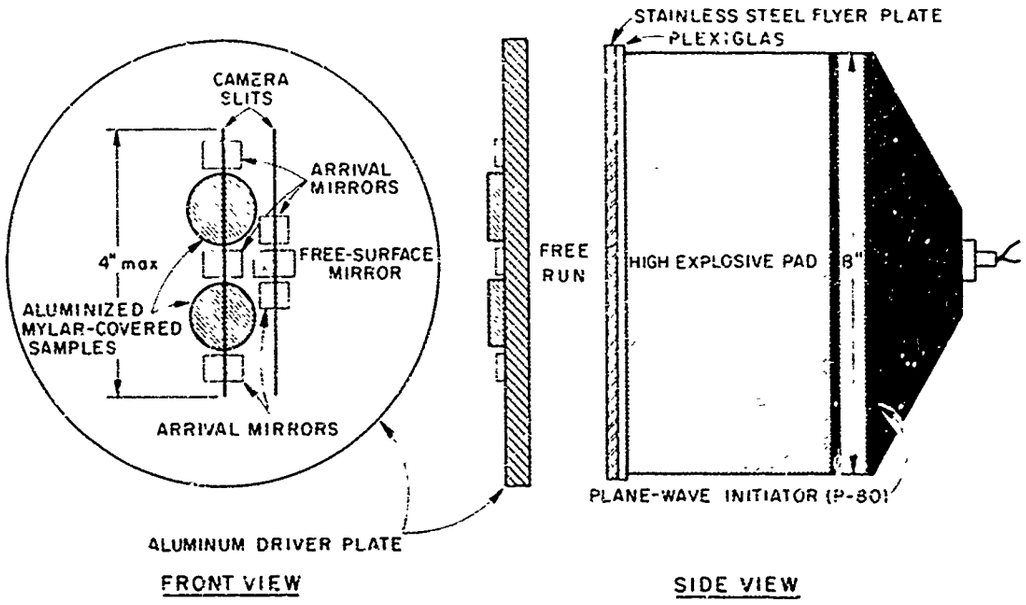

FIG. 2 FLYING PLATE DRIVER ASSEMBLY

surface (Ref. 9). The mirror is mounted so that the slit, the normal to the driver surface, and the normal to the inclined mirror all lie in the same plane, as shown in figure 3. The motion of the free surface destroys the inclined mirror continuously over a small time interval giving an angular cutoff of reflected light intensity on the film (see figure 4b). The mirror angle is chosen so that the velocity of the point of collision is supersonic, thereby eliminating the possibility of a premature cutoff due to stress waves in the mirror. The aluminized surface of the mirror is covered by a thin (1 mil) steel shim to prevent premature cutoff by

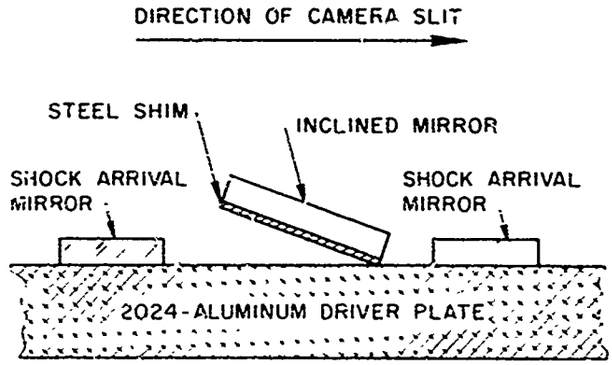

FIG. 3 INCLINED MIRROR TECHNIQUE FOR FREE-SURFACE VELOCITY MEASUREMENT

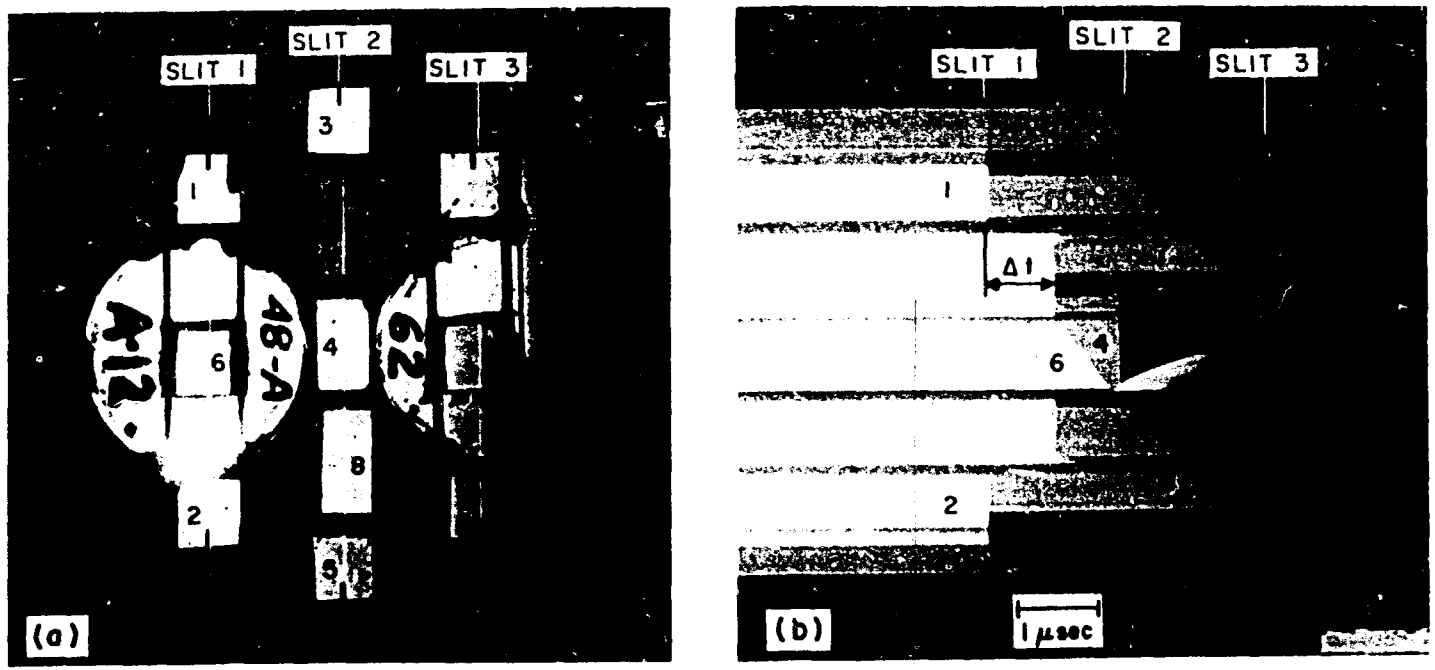

FIG. 4 STILL AND STREAK CAMERA RECORDS OF POROUS ALUMINUM HUGONIOT SHOT

microjetting or by a shock in the ambient gas. The mirrors mounted on the surface on either side of the inclined mirror indicate shock arrival at the free surface and any tilt the shock front may have. Knowledge of the initial angle at which the inclined mirror is mounted, the writing speed of the camera, the magnification of the camera permit calculation of the free-surface velocity from the angle of light cutoff on the film.

Since the plane area on the driver having uniform pressure and simultaneous breakout time was less than 4 inches in diameter, much care was used in layout of samples and free-surface mirrors. Samples were mounted at the same distance from shot center as the driver-state inclined mirrors in order to minimize the effect of radial pressure variation. A typical streak camera record is shown in figure 4. Figure 4a is a still picture of the shot face showing the mirrors with an image of the three streak camera slits exposed over them. Slits 1 and 3 record data from the two samples being studied. On slit 1 (slit 3 is identical), mirrors 1 and 2 are on the driver and record the arrival time of the incident shock at the driver-sample interface. The aluminized Mylar on the circular sample records the arrival of the shock at the sample free surface. Mirror 6 is an inclined mirror mounted to measure the sample free-surface velocity in the manner just described. The free-surface velocity of the aluminum driver is measured on slit 2 by inclined mirrors 7 and 8 while mirrors 3, 4, and 5 are on the driver surface to detect shock arrival and tilt.

The streak camera record from this shot is shown in figure 4b. From slit 1 (and similarly for slit 3) the transit time Δt of the shock through the sample and the inclined mirror cutoff yielding sample free-surface velocity are obtained. From slit 2 the inclined mirror cutoffs yielding driver free-surface velocity are determined.

To reduce extraneous shock light a methane atmosphere surrounded the samples. This proved particularly effective on multiple slit shots.

Similar techniques were used in obtaining high pressure data by double shocking of initially porous aluminum. A small tungsten block was placed over half of the sample and two slits observed the sample. One of the slits recorded the shock velocity through the sample in the manner just described while the other slit, observing the half of the sample covered by tungsten, recorded the free-surface velocity of the tungsten. A third slit recorded the 2024 aluminum driver free-surface velocity just as did slit 2 in figure 4. The free-surface velocity of the driver and the shock

velocity through the sample yield the state behind the initial shock in the sample just as before. Upon reaching the sample-tungsten interface, the initial shock is transmitted as a shock into the tungsten and reflected as a second shock back into the sample. A measurement of the free-surface velocity of the tungsten together with the Hugoniot of tungsten as determined by McQueen and Marsh (Ref. 10) yield the state behind the transmitted shock in the tungsten. Because of continuity of pressure and particle velocity across an interface, the same pressure-particle velocity state exists behind the reflected wave in the sample. The final specific volume and energy behind the reflected wave may then be calculated by appropriately applying the jump conditions across the reflected shock.

b. Experiments using Preheated 1060 Aluminum

Solid 1060 aluminum samples were heated to temperature in excess of 500°C and then impacted by an explosively accelerated brass plate. Measurements of shock velocity through the sample and of the impact velocity suffice to determine a Hugoniot point for the sample if the Hugoniot of the flyer plate is known. The experimental arrangement for studying heated samples is shown in figure 5. Two samples of 1060 aluminum, one to be heated and the other as a cold control sample, are mounted in an aluminum base plate such that the flyer plate strikes the samples directly. The sample to be heated (on the left in figure 5) is supported in a quartz enclosure to insulate it thermally from the base plate. It is heated by a resistance-wire heating element and the temperatures of both the hot and cold samples are monitored by thermocouples as shown. The face of the shot is viewed through the slits of the streak camera. Using the polished surfaces of the samples to reflect light from an argon light source, the shock velocity is determined by recording the time of arrival of the shock at two thicknesses on the sample in much the same manner as with the porous samples. The free-surface velocity is determined by measuring its time of flight across the central gap to a quartz mirror.

Independent measurements of the flyer plate velocity are made by two sets of mirrors mounted in the flight space on the same radius as the samples. The successive destruction of the reflectivity of the central mirror and then the two outer mirrors of each set gives the time of flight over a 5/32-inch gap just prior to flyer-sample impact.

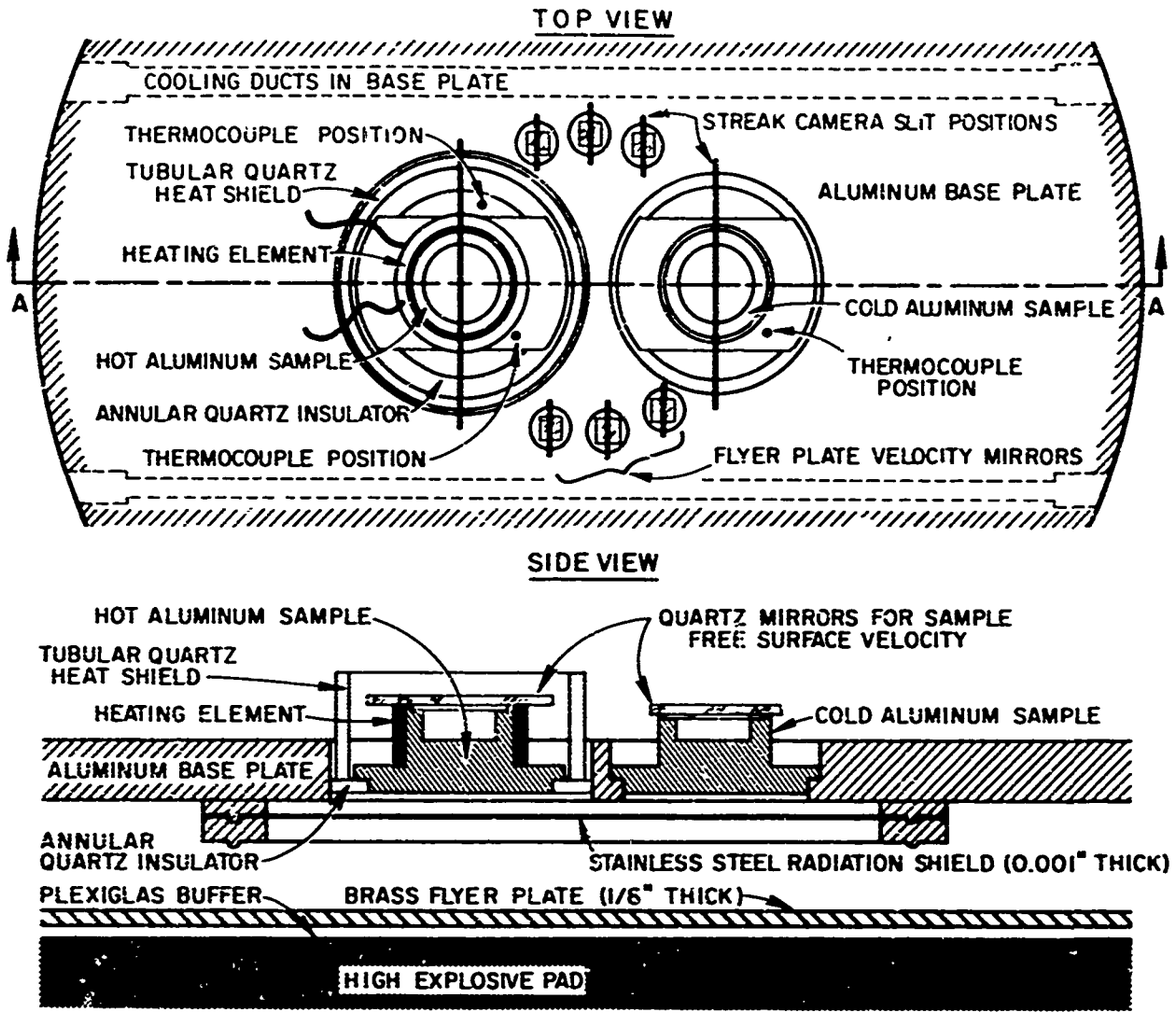

FIG. 5 EXPERIMENTAL ASSEMBLY FOR FIRING PREHEATED SAMPLE

Directly behind the base plate is a 0.001-inch-thick brass or stainless steel radiation shield. It was found desirable in two of the shots to include this heat shield to prevent excessive heating of the flyer plate and the explosive pad. The flyer plate of 1/8-inch brass was accelerated over a 1-inch free run. Brass was used in these experiments since extensive Hugoniot data on brass are available from the work of McQueen and Marsh (Ref. 10). Prior to firing, the entire assembly was pumped down to pressures below 5 μHg.

3. SAMPLE PREPARATION

To prepare the samples, aluminum powder of high purity was pressed in steel rings to the desired density. The values of porosity n, defined by $n = \rho_0/\rho_\infty$ where ρ_0 is crystal density and ρ_∞ is the apparent density, were set at 1.4, 1,7, and 2.0.

The commercial aluminum powder (Reynolds # 40 Atomized Powder) had an average particle size of 30 ± 5 microns but the rather large range of particle sizes made sieving necessary. The samples of porosity $n = 1.4$ and $n = 1.7$ were made from powder which was passed through a # 65 mesh sieve (208-micron openings). In order to press samples of porosity $n = 2.0$ that were strong enough to be handled, it was necessary to use a larger particle size. These samples were made from powder which passed through a # 50 mesh sieve (300-micron openings) but not through a # 65 mesh sieve. None of the samples required sintering.

No experiments have been performed on this project to evaluate the effect of particle size on shock wave propagation in porous aluminum. Russian workers (Ref. 6) made such studies on porous copper and lead and concluded that, in the 100-300 kbar range, changing the particle size from 0.5 μ to 100 μ did not affect the shock velocity.[3] It would seem that particle size would be a significant variable in the low pressure region where compaction of the porous structure is incomplete. However, no experiments have been performed to evaluate the effect of particle size on wave shape or on the approach to equilibrium in the pressure range of interest here. Both theoretical and experimental studies of this problem are needed to establish the validity of using porous materials to attain high temperature-low compression states by shock wave techniques.

To make a sample, a weighed-portion of powder was carefully leveled in a massive steel piston cylinder arrangement which held the steel support ring. After pressing several times to a thickness stop, the sample was removed in its ring and weighed and measured for density and thickness. The uncertainty in the average density of a typical sample was ~0.15 percent. Optical records of shock transit times through the specimens indicated that they were of uniform density. A thickness-to-diameter ratio for the samples was chosen to provide a central region of uniaxial strain (free

[3] However, for the large particles, the shock rise time may be no longer negligible, and thus the question may arise as to what portion of the profile is being detected as "shock arrival."

from edge effects) sufficiently large to perform precise measurements. A typical sample was 3/16-inch thick and 1-1/2 inches in diameter, surrounded by a steel ring (1/8-inch wall thickness) and covered on one side with 0.007-inch-thick aluminized Mylar.

Solid aluminum samples were simply machined and lapped from 1060 aluminum.

The solid and porous Teflon samples were obtained from Avco Corporation (for description of preparation, see Ref. 11), in the form of disks nominally 2 inches in diameter and 1/2-inch thick. They were sawed, ground, and dry lapped to size (nominally 3/16-inch thick) and their porosity was determined by direct measurement of dimensions and weights. Teflon sample densities are shown in Table I.

Table I

TEFLON SAMPLE MEASUREMENTS

SAMPLES[a]	THICKNESS (inches)	INITIAL DENSITY (g/cm^3)
2-A	0.1870	2.1639 ± 0.0046[c]
2-B	0.1859	2.1697 ± 0.0035[c]
6	0.4949[b]	1.472
10	0.4944[b]	1.489
10-A	0.1874	1.525
10-B	0.1909	1.518
8	~0.4911[b]	1.511
9	~0.4926[b]	1.487
1-A	0.1885	0.783
1-B	0.1742	0.778

a. Slices of as-received samples indicated by letter on sample number

b. Dimensions of each as-received sample varied by several mils. Average values are given.

c. A value of $\rho_0 = 2.1668\ g/cm^3$ was used in calculating the porosity α.

SECTION IV

EXPERIMENTAL RESULTS

1. ALUMINUM DATA

The measured free-surface velocities of the 2024 aluminum driver plates and the measured shock and free-surface velocities of the solid and porous aluminum samples are presented in Table II. The pressure-particle velocity

Table II

SOLID AND POROUS ALUMINUM SHOCK DATA

SHOT NO.	2024 DRIVER FREE-SURFACE VELOCITY (mm/μsec)	SPECIMEN[a]		
		Initial Density (g/cm^3)	Shock Velocity (mm/μsec)	Free-Surface Velocity (mm/μsec)
		n = 1.0		
11,470	2.89	2.70	7.31	2.97
11,570	3.60	2.70	7.75	--
11,563	5.03	2.70	8.77	--
11,460	5.35	2.70	9.06	5.42
11,562	5.61	2.70	9.13	--
		n = 1.4		
11,477	2.89	1.93	5.98	3.23[b]
10,591	5.07[c]	1.92	7.15	5.43
10,592	5.86	1.92	7.79	5.93
		n = 1.7		
11,155	3.56	1.59	5.43	3.96[b]
11,286	3.96	1.59	5.82	4.14[b]
11,062	4.02	1.59	5.93	4.53
10,876-1	4.67	1.59	6.58	5.21
10,876-2[a]	4.67	1.59	6.50	5.25
10,926	4.97	1.58	6.83	5.53
11,330	5.04	1.59	6.90	5.52
10,591	5.07[c]	1.58	6.91	5.25[b]
10,694	5.43	1.59	7.29	5.95
11,305	5.72	1.58	7.49	--
10,592	5.86	1.58	7.55	6.24
		n = 2.0		
11,155	3.56	1.35	5.09	4.51[b]
11,286	3.96	1.35	5.57	4.16[b]
11,062	4.02	1.35	5.64	5.11
10,926	4.97	1.35	6.72	6.08
11,330	5.04	1.35	6.79	5.84[b]
10,894	5.43	1.35	7.16	6.85
11,379	5.84	1.35	7.29	--
11,305	5.72	1.35	7.32	--

[a] All specimens were nominally 3/26-inch thick, except for the 3/8-inch specimen of Shot No. 10,876-2.

[b] Aluminum shim on free surface.

[c] Adjusted value (see text).

states in the samples were obtained through an impedance match solution using the 2024 aluminum as a standard, as described in Section III. The 2024 aluminum Hugoniot and release cross curves were obtained from Dr. R. G. McQueen of the Los Alamos Scientific Laboratory. The processing of the porous aluminum data consisted of first plotting the specimen shock velocity against the driver plate pressure that was inferred from the measured free-surface velocity (using the LASL cross curves). This plot of primary data (not included in this report) served as an initial check on the scatter in the data. The data for each of the porosities 1.7 and 2.0 defined a smooth curve. The data for porosity 1.4 were not as abundant as for the other porosities. In one shot (No. 10,591), the record yielding the free-surface velocity of the driver plate was ambiguous. Therefore, the point for the sample of porosity 1.7 was made to lie on the shock velocity-driver pressure curve which was well defined by the other data points. In so doing, the point for the 1.4 porosity sample was brought into a position consistent with a smooth curve through the remaining points.

The pressures, particle velocities, volumes, and energies computed from the primary data by use of the impedance match technique and the Rankine-Hugoniot jump conditions are presented in Table III. Some of the data reported in Tables II and III differ slightly from those reported earlier in the progress reports. The data have been rechecked for errors in calculations, and questionable shot records have been reanalyzed. The present results reflect the changes arising in the reexamination.

The porous aluminum data are plotted on a shock velocity-particle velocity diagram in figure 6. Plotted on the same figure are some porous aluminum data obtained by Avco (Ref. 11). Straight lines represent all the data quite well for $\alpha = 2.0$ and $\alpha = 1.7$ over the range investigated. The three points for $\alpha = 1.4$ lie on a straight line. The three highest pressure Avco points for $\alpha = 1.5$ lie between the lines for $\alpha = 1.7$ and $\alpha = 1.4$ but indicate a different slope. The two lower Avco $\alpha = 1.5$ points appear questionable (indicated by parentheses) as they imply pressure-volume states which are quite scattered from the remainder of the data.

Representation of shock data for porous material by a linear shock velocity-particle velocity relationship is invalid for the purpose of extrapolation to lower pressures. The relationship

$$U = C + Su \qquad (41)$$

Table III

SOLID AND POROUS ALUMINUM HUGONIOT DATA

SHOT NO.	INITIAL VOLUME (cm^3/g)	SHOCK VELOCITY (mm/μsec)	PARTICLE VELOCITY (mm/μsec)	PRESSURE (kbar)	FINAL VOLUME (cm^3/g)	COMPRESSION[a] $\mu = \rho/\rho_0 - 1$	INTERNAL ENERGY CHANGE (10^9 ergs/g)
11,477	0.370	7.31	1.45	286	0.297	0.250	10.65
11,570	0.370	7.75	1.80	377	0.284	0.302	16.21
11,563	0.370	8.77	2.46	583	0.266	0.391	30.31
11,460	0.370	9.06	2.58	633	0.265	0.396	33.23
11,562	0.370	9.13	2.71	667	0.260	0.423	36.56
11,477	0.519	5.08	1.88	184	0.328	0.128	17.57
10,591	0.520	7.15	3.03	418	0.299	0.237	46.18
10,592	0.521	7.79	3.42	511	0.293	0.262	58.25
11,155	0.629	5.43	2.43	210	0.347	0.066	29.61
11,286	0.631	5.82	2.67	246	0.341	0.085	35.67
11,062	0.629	5.93	2.69	254	0.344	0.075	36.19
10,876-1	0.630	6.58	3.05	319	0.338	0.094	46.57
10,876-2	0.629	6.50	3.06	316	0.333	0.111	46.76
10,926	0.631	6.83	3.20	347	0.335	0.104	51.35
11,330	0.631	6.90	3.25	355	0.334	0.107	52.72
10,591	0.633	6.91	3.26	356	0.334	0.107	53.22
10,894	0.630	7.29	3.44	397	0.333	0.111	58.95
11,305	0.631	7.49	3.58	426	0.330	0.121	64.11
10,592	0.635	7.55	3.66	436	0.327	0.131	67.14
11,155	0.741	5.09	2.58	177	0.365	0.0136	33.19
11,286	0.741	5.57	2.82	212	0.364	0.0164	33.85
11,062	0.741	5.64	2.85	218	0.367	0.0081	40.76
10,926	0.741	6.72	3.37	305	0.369	0.0027	56.73
11,330	0.740	6.79	3.41	313	0.369	0.0027	58.06
10,894	0.741	7.16	3.60	348	0.362	0.0054	64.90
11,379	0.744	7.29	3.85	377	0.351	0.0541	74.08
11,305	0.741	7.32	3.78	373	0.360	0.0277	71.05

[a] Values of μ based on crystal density $\rho_0 = 2.70$ g/cm^3.

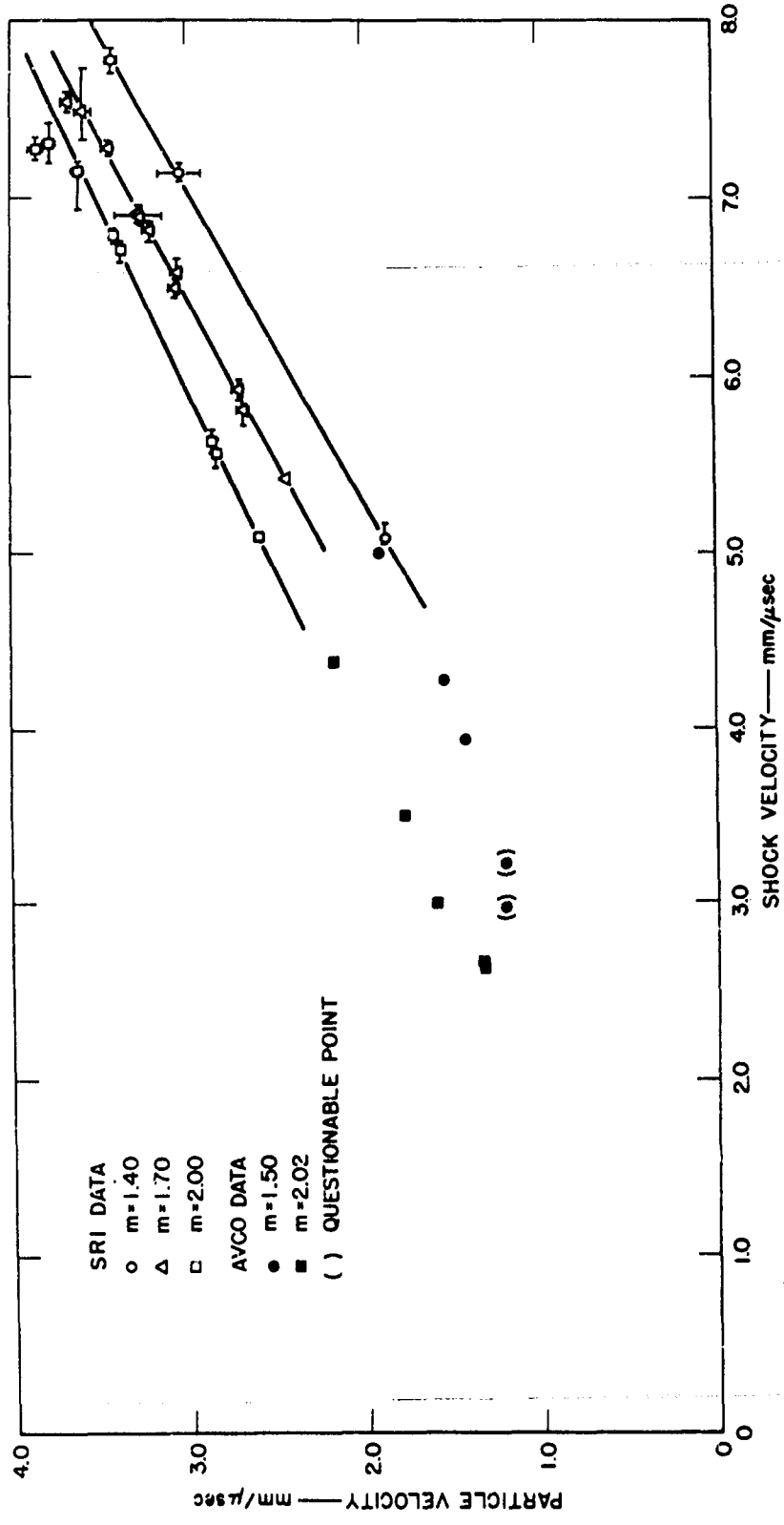

FIG. 6 PARTICLE VELOCITY vs. SHOCK VELOCITY FOR POROUS ALUMINUM

where C and S are constants, implies a pressure-volume Hugoniot given by

$$P = \frac{\frac{\rho_0}{m} C^2 [1 - V/mV_0]}{[1 - S(1 - V/mV_0)]^2} \qquad (42)$$

where V_0 and ρ_0 are the initial specific volume and density, respectively, of the solid material. The pressure vanishes at mV_0 in Eq. (42), rather than at V_0 as it must in a model that assumes zero crushing strength of a porous solid. Although the crushing strength is not actually zero, the low pressure extrapolation of Eq. (39) indicates a much higher pressure and greater curvature of the Hugoniot than is consistent with very low pressure experiments carried out in this laboratory on another project (Ref. 12).

The data have been plotted in the pressure-volume plane in figure 7. Shown also on the figure are the Hugoniot of solid aluminum from Al'tshuler and the 0°K isotherm from the McCloskey program (Ref. 13). Measurements of the density of the solid 1Q60 aluminum yielded a value of 2.70 g/cm^3. The Russians quote a value of 2.71 g/cm^3 for the density of aluminum used in their experiments. To make their Hugoniot comparable to the data reported here each of their volumes at a given pressure was changed by a factor 2.71/2.70. This maintains the shape of the curve but translates it slightly toward the right, *i.e.*, larger volumes. During the course of studying aluminum, it was also found that the Los Alamos Hugoniot curve for 2024 aluminum could be made to agree quite closely with the Soviet Hugoniot for pure aluminum by translating the 2024 curve to the right by a factor of 2.78/2.71, the ratio of the initial densities. Smooth curves have been drawn through the porous aluminum data. These curves do not represent analytical fits to the data nor are they obtained from the straight lines of figure 6. They have been extrapolated to zero pressure and crystal volume (dashed portion), so as to be consistent with a negligible crushing strength. In the absence of data at very low pressure, there appears to be no *a priori* justification to make any other type of extrapolation.

The two highest pressure points on the Hugoniot for porosity $m = 2$ have not been weighted in drawing the curve through those data. The evidence suggests that the abrupt change in slope indicated by those points is not a real property of the aluminum but rather an effect of shock attenuation.

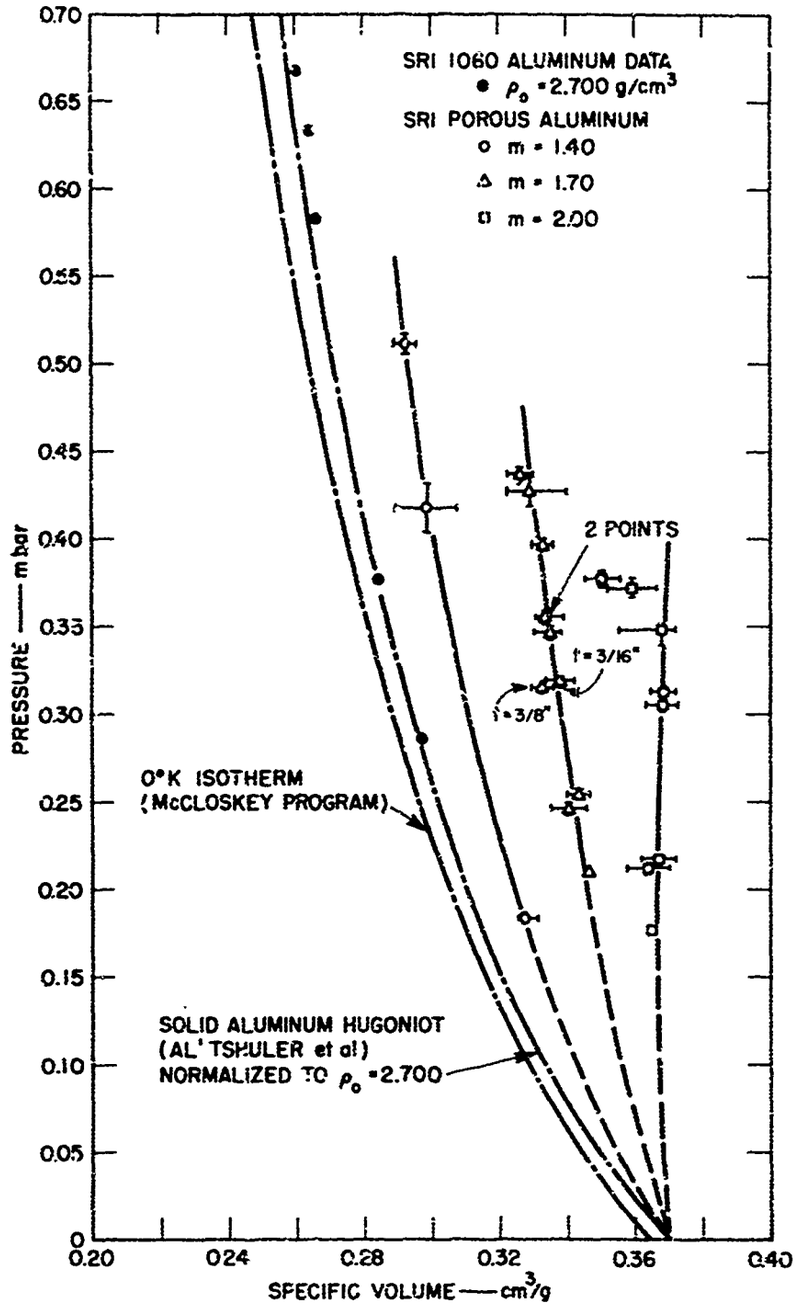

FIG. 7 HUGONIOTS FOR ALUMINUM

The attenuation is due to the overtaking of the shock by the rarefaction from the back surface of the flyer plate. There is no conclusive proof that this is the case, but calculations based on sound speeds in solid aluminum indicate that, in the high-pressure porous aluminum experiments, the margin of safety for obtaining data free from attenuation effects is quite small. In figure 7 two points on the Hugoniot of porosity $m = 1.7$ are labeled $t = 3/16$ inches and $t = 3/8$ inches, where the t refers to the sample thickness. Both samples were mounted on the same type of driver plate. The driver under the 3/8-inch sample was struck by a 3/16-inch flyer plate while that of the 3/16 sample was struck by a 1/8-inch flyer. Attenuation will be most likely for the smallest ratio of specimen thickness to flyer thickness, *i.e.*, for the thickness sample in the present case. Indeed, it appears that attenuation did affect the thicker sample. The few experiments performed on this project to attempt to evaluate shock attenuation effects indicate a need for more studies in shock wave propagation in porous materials.

The uncertainties in each of the points in figure 7 were calculated by a computer program which takes into account uncertainties in measured wave and free-surface velocities and in the initial density of the sample.

According to Eq. (15), if the Grüneisen ratio is dependent only upon volume, it represents the ratio of the thermal pressure to the thermal energy density

$$\Gamma(V) = V\frac{P - P_c(V)}{E - E_c(V)} = V\frac{P_{th}}{E_{th}} \tag{15}$$

where the subscript "th" means thermal. In cases where Grüneisen's ratio is a function of volume plus another independent variable, Eq. (15) is not the Mie-Grüneisen equation of state. However, a parameter λ analogous to the Grüneisen ratio may be defined by

$$\lambda(E,V) = V\frac{P - P_r(V)}{E - E_r(V)} \tag{43}$$

where $P_r(V)$ is some reference curve in the $P - V$ plane and $E_r(V)$ is the energy along that curve. If $P_r(V)$ and $E_r(V)$ are the 0°K pressure and energy, then λ is the ratio of the thermal pressure to thermal energy

density. In the limit as the curve $P_r(V)$ is approached at constant volume, $\lambda(E,V)$ approaches $\Gamma(E,V)$, since Eq. (41) approaches the partial derivative which defines $\Gamma(E,V)$.

In earlier quarterly reports (Ref. 14) some values of λ were computed from the experimental data using the Soviet Hugoniot (Ref. 6) for solid aluminum as a reference. Plots of the resulting values against volume indicated a decrease of λ with decreasing volume and increasing energy. It was pointed out that the uncertainties in λ could be as large as 20 percent. It now appears that this estimate of the uncertainty in λ was quite optimistic.

As mentioned earlier, the data have recently been reanalyzed. The positions of the aluminum Hugoniots for porosities $n = 1.7$ and $n = 2.0$ have not been significantly altered. However, the Hugoniot for $n = 1.4$ has been shifted toward the solid Hugoniot, particularly in the low pressure region, due to the addition of a new point (Shot 11,477) and the rejection of Shot 10,590 (because of the poor quality of the film record). The resulting curves are those of figure 7. The values of λ at a given volume were substantially reduced. Since individual points are subject to some scatter and the resulting values of λ are so sensitive to the movement of a Hugoniot point in the $P - V$ plane, it appears reasonable to draw a smooth curve through the data points in the $P - V$ plane and then to compute values of λ from the curve rather than from individual points. It also appears to give λ a more unique value if the 0°K isotherm is used as a reference curve instead of the solid Hugoniot. In this case, $\lambda = VP_{th}/E_{th}$. The 0°K isotherm from the McCloskey program was used.

A plot of the points VP_{th} against E_{th} taken from the Hugoniot curves and 0°K isotherm of figure 7 is shown in figure 8. The curve obtained from Hugoniot $n = 2$ appears to have positive curvature while the curves for $n = 1.0$, 1.4 and 1.7 appear to have negative curvature. The points for $n = 1$ cluster near the origin as thermal pressure and energy are comparatively low along this Hugoniot.

The values of λ calculated from each of the Hugoniot curves for $n = 1.4$, 1.7, and 2.0 are plotted against volume in figure 9 and against thermal energy in figure 9(b). The curves for the Hugoniot $n = 1$ are values computed by the Russians from the 0°K isotherm, using the Slater relation for Γ. It must be emphasized that these values of λ are calculated from the curves drawn through the data and that the drawing of

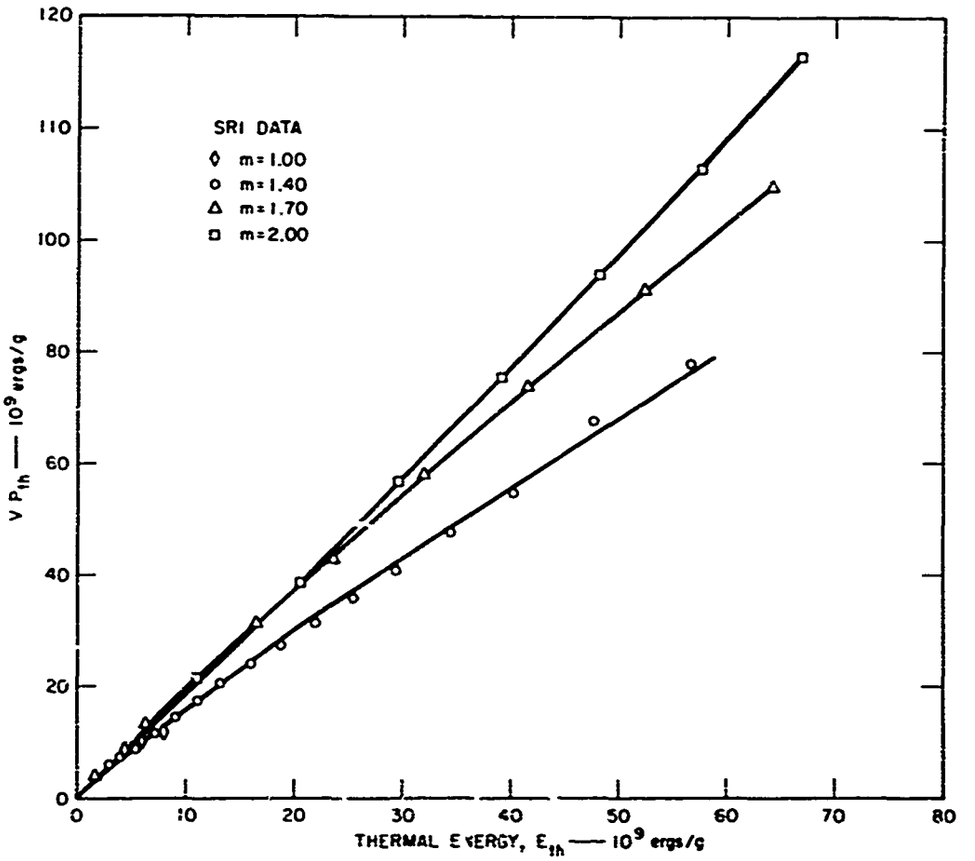

FIG. 8 VOLUME × THERMAL PRESSURE vs. THERMAL ENERGY AT CONSTANT POROSITY

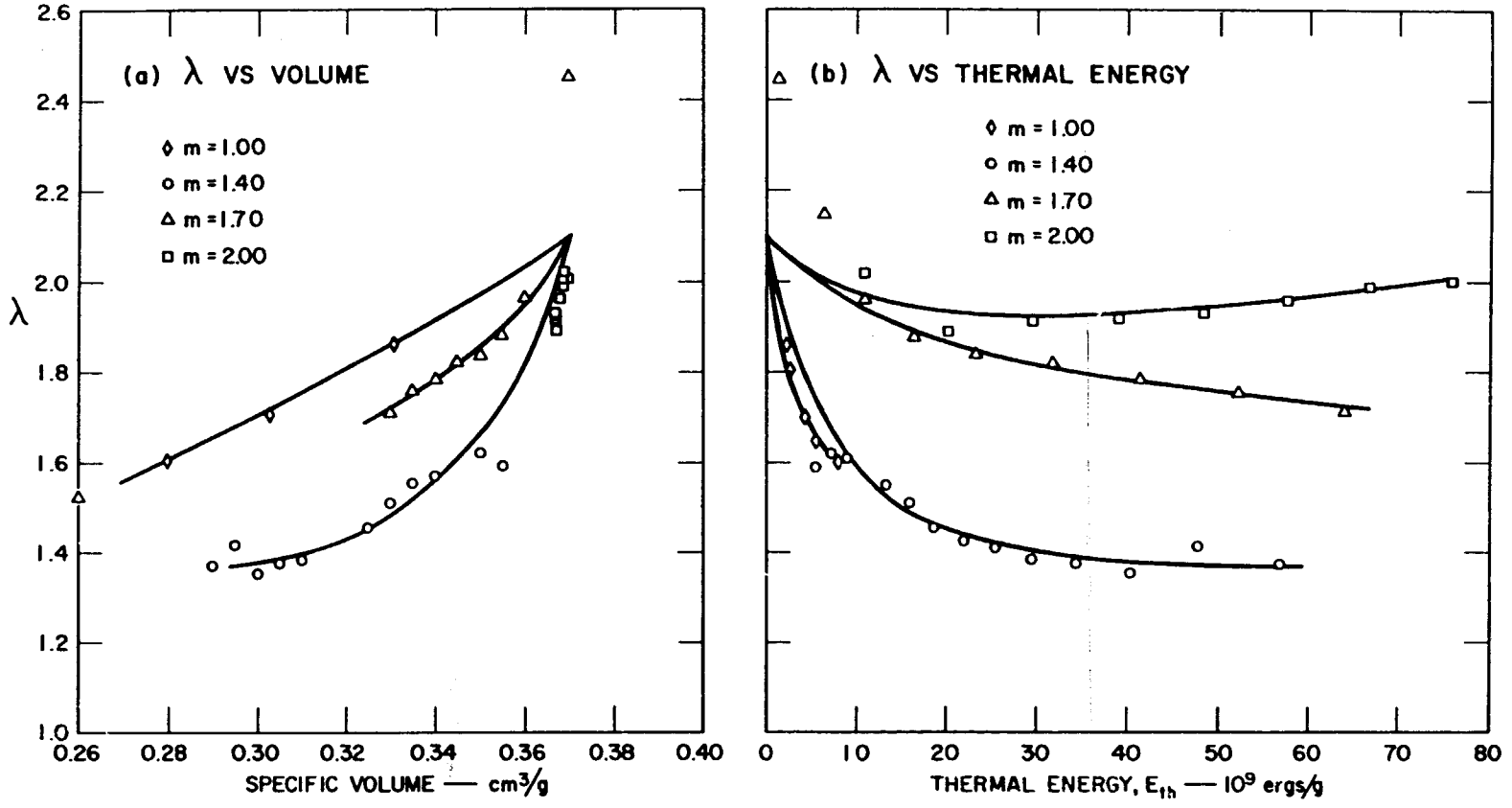

FIG. 9 EFFECTIVE GRÜNEISEN RATIO λ FOR ALUMINUM AT CONSTANT POROSITY

slightly different curves would yield quite different λ values. Also, the curves have been forced to pass through $\lambda = 2.1$ at $V = V_0$ and $P = 0$.[4] The Hugoniot for $s = 1.7$ is the most well defined of the three as it is based on more data. The Hugoniot $s = 1.4$ is the most questionable as it is based upon only three data points. An analysis of the above results was made to see if the dependence on volume and on thermal energy could be resolved in a simple way. To achieve this, curves of λ as a function of volume at constant thermal energy and as a function of thermal energy at constant volume were plotted. The results are shown in figures 10 and 11. A maximum of three points was available for each curve. The minima in the λ vs. E_{th} curves are due to the low values of λ obtained from the $s = 1.4$ Hugoniot. As this Hugoniot is not well defined, no significance can be attached to the minima. It is felt that carrying this analysis further is not warranted with the present quantity of data. Obtaining a large amount of data so that a statistical analysis could be applied appears to be the most meaningful method of truly studying the behavior of Grüneisen's ratio from shock-wave data.

Three high pressure points were obtained by the multiple shock technique using tungsten as a shock reflector. The data are presented in Table IV. The values of λ are calculated from the final shock state. The internal energies of the two highest pressure points are in excess of the sublimation energy. In considering the pressure and energy range covered by these data compared with the single shock data on porous aluminum, the most significant result is the fact that although it does not appear possible to definitely establish the energy and volume dependence of λ, the values obtained do not vary widely and are quite close to the zero pressure value obtained from thermodynamic data.

The Hugoniot data obtained from the experiments in which preheated solid 1060 aluminum samples were used are presented in Table V. For the purpose of studying Grüneisen's ratio as calculated from thermal pressure and energy offsets from the 0°K isotherm, these data are not useful. The offsets in the preheated Hugoniot points from the room temperature Hugoniot of solid 1060 aluminum were too small to be considered significant.

---

[4] At $(P = 0, V = V_0)$, $\lambda \cong \Gamma = V(\partial P/\partial E)_V = VB_T\beta/C_V \cong 2.1$ for aluminum, where B_T is the isothermal bulk modulus and β is the volume coefficient of thermal expansion.

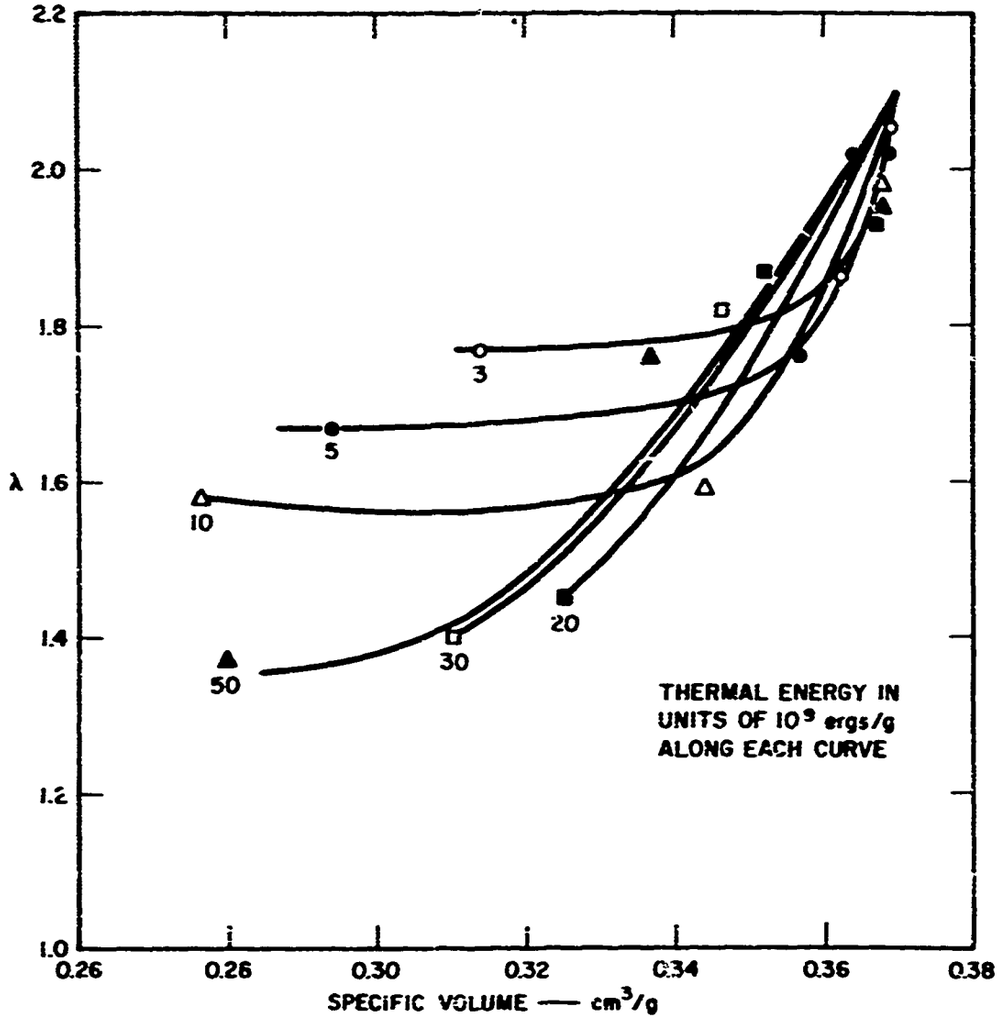

FIG. 10 EFFECTIVE GRÜNEISEN RATIO λ vs. SPECIFIC VOLUME AT CONSTANT THERMAL ENERGY

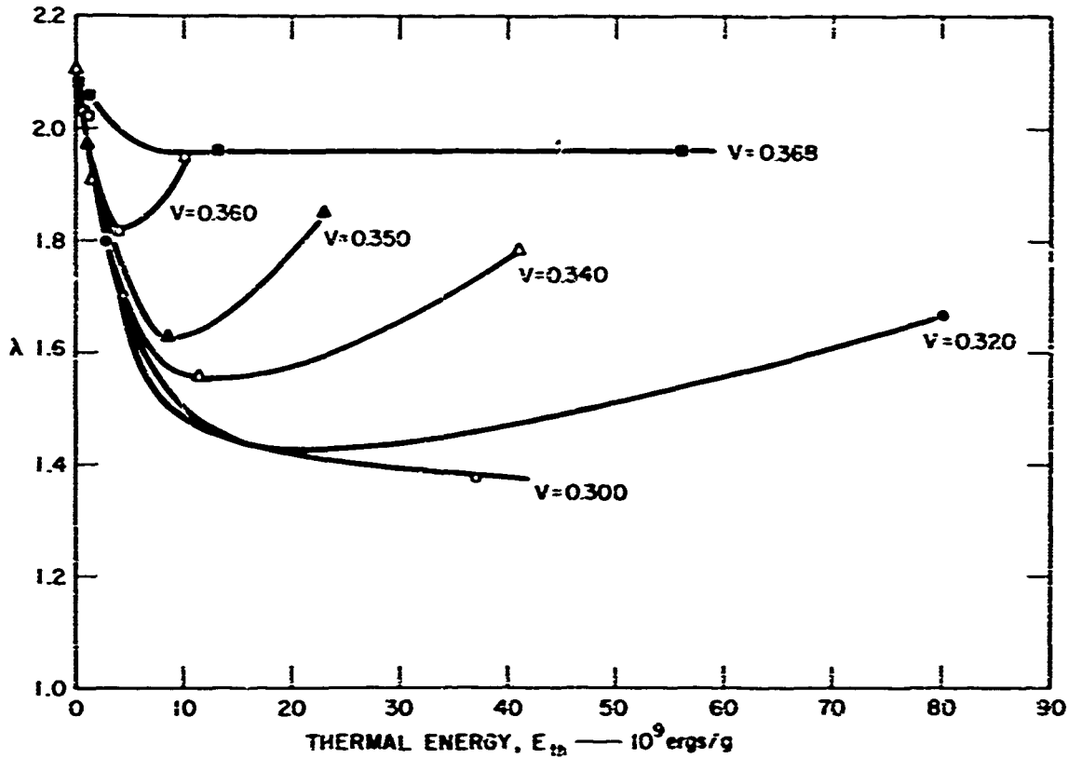

FIG. 11 EFFECTIVE GRÜNEISEN RATIO λ vs. THERMAL ENERGY AT CONSTANT VOLUME

Table IV

DOUBLE SHOCK POROUS ALUMINUM DATA

SHOT NO.	INITIAL VOLUME (cm^3/g)	FIRST SHOCK			SECOND SHOCK			TOTAL ENERGY[a] (10^9 ergs/g)	λ
		Pressure (kbar)	Final Volume (cm^3/g)	Energy Change (10^9 ergs/g)	Pressure (kbar)	Final Volume (cm^3/g)	Energy Change (10^9 ergs/g)		
10,876	0.630	319	0.338	46.57	984	0.270	44.30	92.53	1.90
11,305	0.631	426	0.330	64.11	1,261	0.261	58.20	123.97	1.87
11,305	0.741	373	0.360	71.05	1,244	0.282	63.96	135.77	2.03

[a] $E = \Delta E_1 + \Delta E_2 + 1.66 \times 10^9$ ergs/g.

Table V

HUGONICT DATA FOR PREHEATED AND ROOM TEMPERATURE SOLID 1060 ALUMINUM

T_0 (°C)	SHOCK VELOCITY (mm/μsec)	PARTICLE VELOCITY (mm/μsec)	FREE-SURFACE VELOCITY (mm/μsec)	P_1 (kbar)	V_1 (cm^3/g)	$E_1 - E_0^a$ (erg/g)
542	8.82	2.79	5.47	648	0.264	44.6×10^9
17	8.76	2.77	5.48	656	0.252	38.7×10^9
555	8.56	2.76	5.27	611	0.262	43.3×10^9
17	8.82	2.70	5.14	647	0.257	36.6×10^9
543	8.24	2.23	4.66	475	0.282	30.1×10^9
17	8.14	2.21	4.56	486	0.270	24.3×10^9

[a] Energy increase relative to state $P = 0$, $T = 17°C$.

As a consistency check some Hugoniot points for solid room temperature 1060 aluminum of measured initial density 2.70 g/cm^3 were obtained by the same technique used on the porous samples. The points, shown on figure 7, are in good agreement with the Soviet Hugoniot[5] for solid aluminum at low pressures—and only fair at the highest pressures.

2. TEFLON DATA

Ten data points on solid and porous Teflon (see Table VI) were obtained using the same explosive driver systems and impedance match technique (2024 aluminum standard) as was used in obtaining the porous aluminum

Table VI

SOLID AND POROUS TEFLON DATA

SHOT NO.	ρ_0 (g/cm^3)	$\frac{-}{n}$	U (mm/μsec)	P (kbar)	u (mm/μsec)	V (cm^3/g)	ΔE (10^9 ergs/g)
11,570	0.7828	2.77	4.374	103	2.985	0.4057	44.87
11,563	0.7782		5.646	175.5	3.985	0.3780	79.58
11,562	0.7828		6.086	207.0	4.335	0.3676	94.12
11,570	1.517	1.42	4.909	190.3	2.555	0.5160	32.64
11,563	1.524		6.207	319.0	3.373	0.2995	56.87
11,562	1.517		6.683	371.0	3.66	0.2981	66.97
11,570	2.169	1.00	5.589	269.0	2.215	0.2782	24.58
11,563	2.163		6.830	435.0	2.945	0.2629	43.37
11,460	2.172		7.105	476.0	3.080	0.2608	47.50
11,562	2.163		7.262	504.0	3.29	0.2585	51.35

[5] The shift in the Soviet Hugoniot described earlier is well within experimental error.

data. In figure 12 the shock velocity is plotted against the particle velocity. The data obtained by the Avco Corporation are also included on this graph for comparison. Figure 13 is a plot of the Hugoniot pressure as a function of volume. As with the porous aluminum data, smooth curves have been drawn through the points.

Since there is no theory at the present time as to the equation of state of a plastic, and since the present data are preliminary, it is felt that further analysis should wait until more data are obtained. However, some estimates of the Grüneisen ratio can be made on the basis of the data. In the absence of a 0°K isotherm for Teflon a few values of Γ were computed from the curves drawn through the Hugoniots of porous Teflon using the curve drawn through the Hugoniot of solid Teflon as a reference. The results of these calculations are presented in Table VII. An estimate of Γ_0, Grüneisen's ratio at zero pressure, was made for Teflon based upon available zero pressure data. From the thermodynamic definition of Grüneisen's ratio

$$\Gamma = \frac{VB_T\beta}{C_v} \tag{44}$$

where B_T is the isothermal bulk modulus and β is the thermal expansion coefficient. Values of β and C_v were found to be (Ref. 15)

$$\beta = 16.5 \times 10^{-5}/°C$$

$$C_v = 0.25 \text{ cal/g} \quad (\text{at } 73°C)$$

B_T was estimated from the data of Bridgman to be 43 kbar (Ref. 16). Inserting these values into Eq. (44) yields a value $\Gamma_0 = 0.313$.

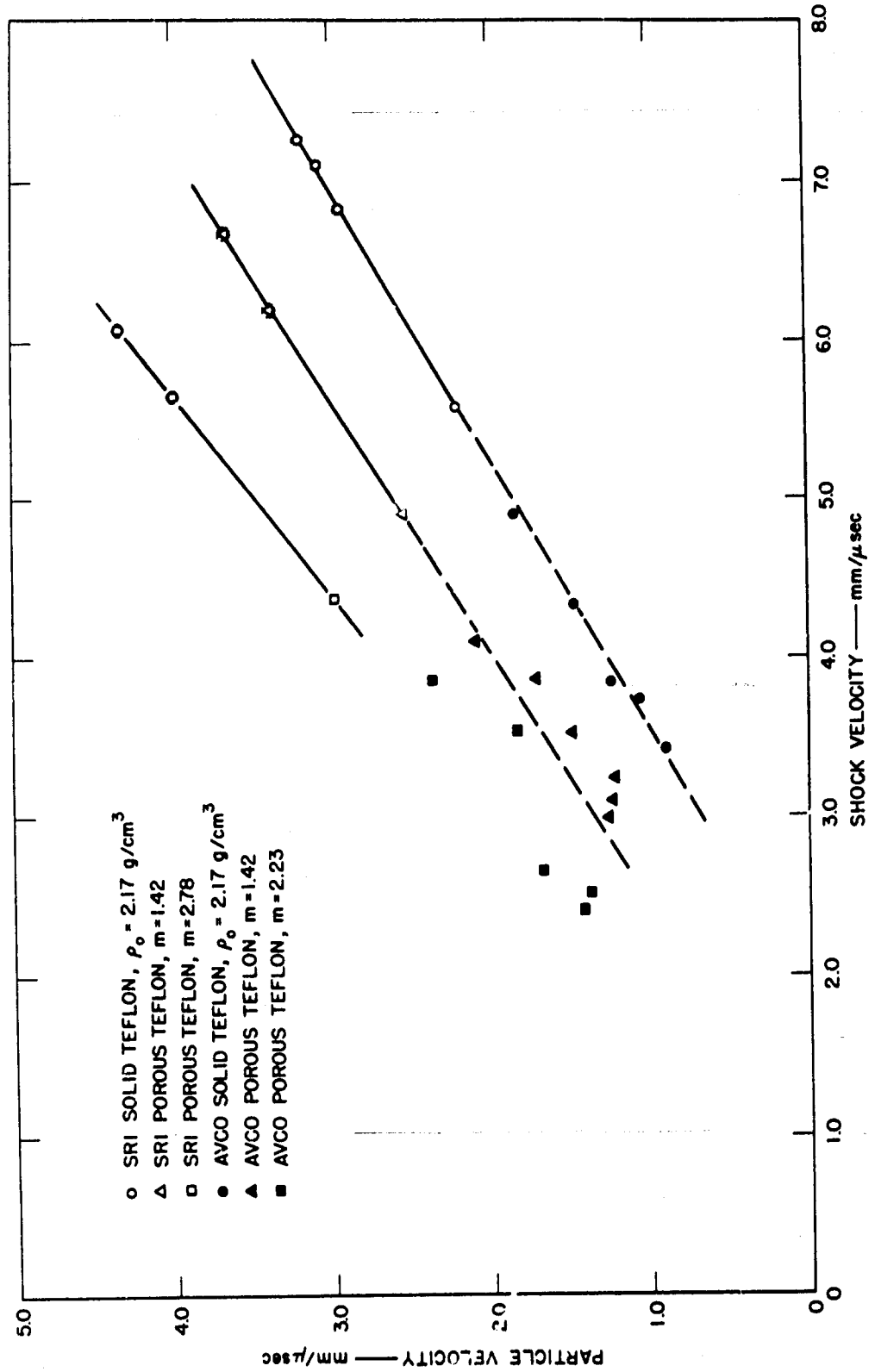

FIG. 12 PARTICLE VELOCITY vs. SHOCK VELOCITY FOR TEFLON

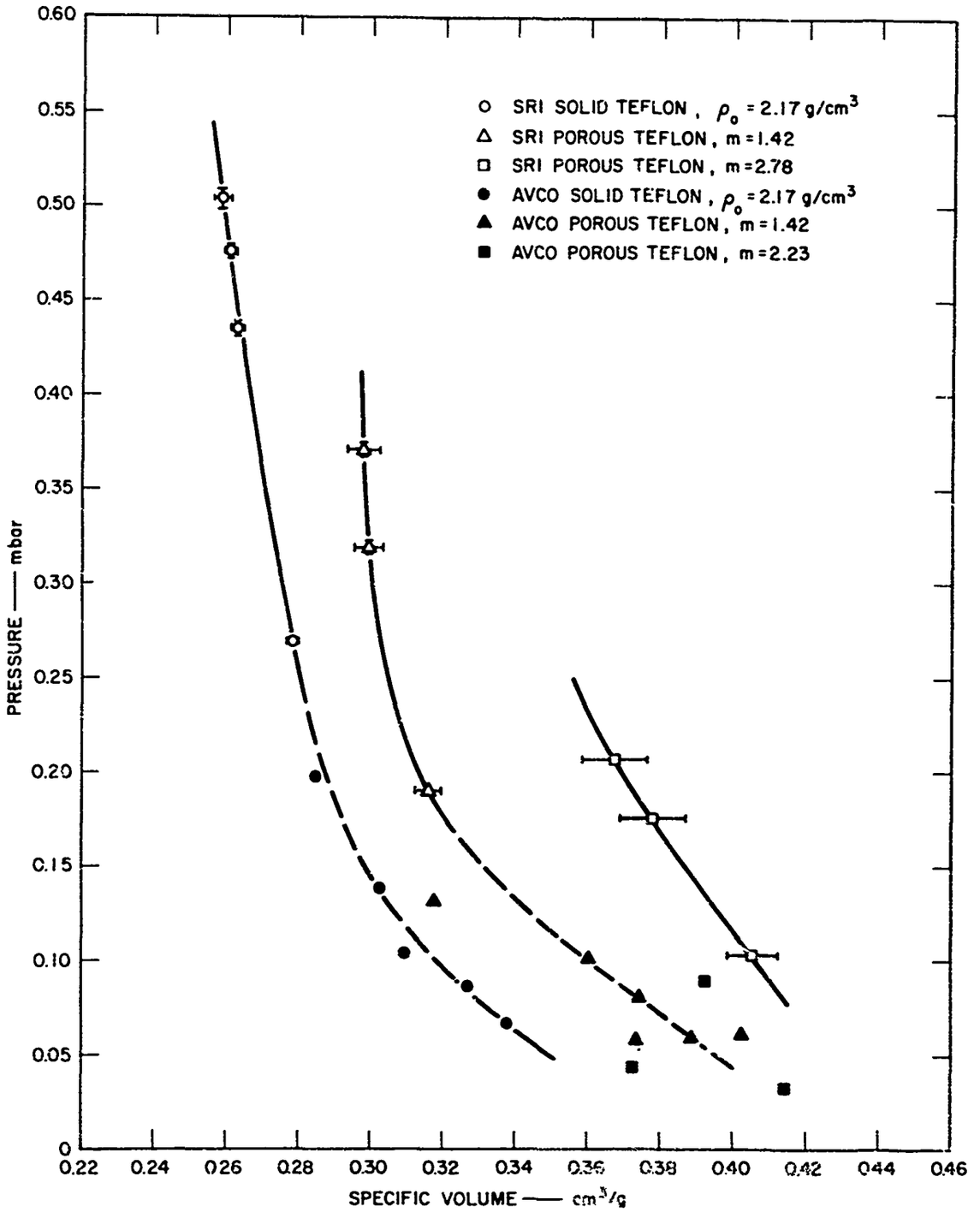

FIG. 13 HUGONIOTS FOR TEFLON

Table VII

CALCULATED VALUES OF λ FOR TEFLON[a]

POROSITY n	POROUS HUGONIOT			λ
	Volume (cm^3/g)	Pressure (kbar)	Energy (10^9 ergs/g)	
1.42	0.310	215	37.18	1.063
1.42	0.340	133	21.0	1.355
1.42	0.370	87	12.4	1.720
1.42	0.400	44	5.63	2.047
2.78	0.370	199	91.04	0.678
2.78	0.400	127	56.2	0.783

[a] Hugoniot of Teflon n = 1.0 used as a reference curve.

REFERENCES

1. Slater, J. C., *Introduction to Chemical Physics*, McGraw-Hill Book Co., New York, 1939.

2. Dugdale, J. S. and D. K. C. MacDonald, Phys. Rev. 89, 832 (1953).

3. Rice, M. H., R. G. McQueen, and J. M. Walsh, *Compression of Solids by Strong Shock Waves*, Solid State Physics, Vol. 6. F. Seitz and D. Turnbull, eds., Academic Press, New York, 1958.

4. Al'tshuler, L. V., K. K. Krupnikov, B. N. Ledenev, V. S. Zhuchikkin, and M. I. Brazhnik, Soviet Physics, JETP 7, 606 (1958).

5. Krupnikov, K. K., M. I. Brazhnik, and V. P. Krupnikova, Soviet Physics, JETP 15, 470 (1962).

6. Kormer, S. B., A. I. Funtikov, V. D. Urlin and A. N. Kolesnikova, Soviet Physics, JETP 15, 477 (1962).

7. Anderson, G. D., *A Summary of the Soviet Papers on the High Pressure Equation of State of Metals*, AFWL TR-65-130, Stanford Research Institute, September 1965.

8. McQueen, R. G., Los Alamos Scientific Laboratory, private communication.

9. Doran, D. G., *Measurement of Shock Pressures in Solids*, High Pressure Measurement, A. A. Giardini and E. C. Lloyd, eds., Butterworth, Inc., Washington, D. C., 1963.

10. McQueen, R. G. and S. P. Marsh, J. Appl. Phys. 31, 1253 (1960).

11. Morgan, D. T., M. Rockowitz, and A. L. Atkinson, *Measurement of the Grüneisen Parameter and the Internal Energy Dependence of the Solid Equation of State of Aluminum and Teflon*, AFWL TR-65-117, Avco Corporation, September 1965.

12. Linde, R. K., Stanford Research Institute, private communication.

13. McCloskey, D. J., *An Analytic Formulation of Equations of State*, RM-3905-PR, The Rand Corporation, February 1964.

14. Anderson, G. D., *Equation of State of Solids*, QPR No. 2, SRI Project GSU-5057, Stanford Research Institute, November 9, 1964.

15. *Technical Data on Plastics*, Manufacturing Chemists Association, Inc., Washington, D.C., 1957.

16. Bridgman, P. W., Proc. Am. Acad. Art. Sci., 76, 71 (1948); Collected Papers, Vol. VI.

Unclassified

Security Classification

DOCUMENT CONTROL DATA · R&D

(Security classification of title, body of abstract and indexing annotation must be entered when the overall report is classified)

1 ORIGINATING ACTIVITY (Corporate author) Stanford Research Institute Menlo Park, California	2a REPORT SECURITY CLASSIFICATION Unclassified 2b GROUP

3 REPORT TITLE

EQUATION OF STATE OF SOLIDS: ALUMINUM AND TEFLON

4. DESCRIPTIVE NOTES (Type of report and inclusive dates)

Final Report 15 May 1964 through 14 July 1965

5. AUTHOR(S) (Last name, first name, initial)

Anderson, G. D.; Doran, D. G.; and Fahrenbruch, A. L.

6. REPORT DATE	7a. TOTAL NO. OF PAGES	7b. NO. OF REFS
December 1965	58	16

8a. CONTRACT OR GRANT NO. AF29(601)-6409 b. PROJECT NO. 5710 c. Subtask: 15.018 d.	9a. ORIGINATOR'S REPORT NUMBER(S) AFWL-TR-65-147 9b. OTHER REPORT NO(S) (Any other numbers that may be assigned this report) SRI Project GSU-5057

10. AVAILABILITY/LIMITATION NOTICES

Distribution of this document is unlimited.

11. SUPPLEMENTARY NOTES	12. SPONSORING MILITARY ACTIVITY
	Air Force Weapons Laboratory (WLRP) Kirtland AFB, New Mexico 87117

13. ABSTRACT

Pressure, volume, and energy equation of state data obtained using shock wave techniques are presented for aluminum and Teflon. Solid aluminum samples initially at room temperature or preheated to near melting, and porous aluminum samples at room temperature, were studied over a pressure range of 200 to 1200 kbar. It was found that the largest variations of volume and energy could be achieved using porous samples. Values of Gruneisen's ratio estimated from values of the thermal pressure and thermal energy range from 2.1 to 1.37. Due to the sensitivity of Gruneisen's ratio to the Hugoniot data, it is not possible to formulate its energy or volume dependence conclusively at the present time. Of greatest significance is the fact that it does not vary widely.

Solid and porous Teflon samples were studied over a pressure range of 100 to 500 kbar. Hugoniot curves drawn on the basis of the ten data points obtained indicate a variation of Gruneisen's ratio from about 0.7 to 2.0.

DD FORM 1 JAN 64 1473

Unclassified

Security Classification